

New Semiconducting Polymer Based on Benzo[1,2-b:4,5-b']diselenophene Donor and Diketopyrrolopyrrole/Isoindigo Acceptor Unit: Synthesis, Characterization and Photovoltaics

Zhongjie Xu,^a Guozheng Shi,^a Jianyu Yuan,^a Emily Glenn,^b Hai-Qiao Wang,^{*,a} and Wanli Ma^{*,a}

^a Institute of Functional Nano & Soft Materials (FUNSOM), Jiangsu Key Laboratory for Carbon-Based Functional Materials & Devices, Soochow University, Suzhou, Jiangsu 215123, China

^b University of Waterloo, 200 University Avenue West, Waterloo Ontario, N2L3G1, Canada

Two new D-A type polymers PBDSe-DPP and PBDSe-ID were synthesized to explore new ideal semiconducting polymers, by conjugating acceptor unit diketopyrrolopyrrole/isoindigo to a donor unit benzo[1,2-b:4,5-b']diselenophene, which is designed by substituting the sulfur atom with a selenium atom in the benzo[1,2-b:4,5-b']dithiophene. The thermal, optical, electrochemical, photoelectric and photovoltaic properties of the two polymers were studied systematically. Relatively high open circuit voltage (0.7 and 0.75 V) and fill factor (>65%) were demonstrated for both polymers. Huge increase (by 64% and 120%) of the short circuit current density was achieved for both polymer based devices by using additive compared to the corresponding reference without additive, resulting in decent power conversion efficiency of 3.7% and 2.5% respectively with only simple optimizing consideration. We believe this class of BDSe polymer possesses a good potential to be alternatives of active material for photovoltaic applications.

Keywords semiconducting polymer, benzo[1,2-b:4,5-b']diselenophene, synthesis, characterization, photovoltaics

Introduction

Polymer solar cells (PSCs) have gained considerable attention during the past decades due to the fact that they are inexpensive, lightweight, easily solution-processable and capable of flexible fabrication.^[1-3] Bulk-heterojunction PSCs consisting of interpenetrating polymer donor and fullerene acceptor nanoscale networks offer a competitive approach to efficient and cost-effective solar energy technology.^[4-9] To achieve a high efficiency for PSCs, the biggest challenge at molecular level is to develop an ideal p-type conjugated polymer which possesses simultaneously the following properties: sufficient solubility for processing and miscibility with a n-type material, low band gap for broad absorption and strong light absorption coefficient to capture as many solar photons as possible, and reasonable high hole-mobility for efficient carrier transport.^[10-13]

As an electron-rich donor unit, benzo[1,2-b:4,5-b']dithiophene (BDT) has been used to synthesize donor-acceptor (D-A) type low band gap polymers due to its ability to promote polymer's planarity, molecular π - π stack and charge carrier mobility,^[14-16] which is consid-

ered one of the most effective building-blocks for ideal polymers for efficient PSCs.^[15,17,18] On the other hand, benzo[1,2-b:4,5-b']diselenophene (BDSe) donor unit obtained by using electron-rich selenophene to substitute the thiophene moiety, has also been developed as it can lower the band gap of polymers.^[19,20] Besides that, the heavier Se atom can improve the carrier mobility between molecules as the enhanced inter-chain transfer integrals.^[19,21,23] And moreover, selenophene-based copolymers show higher absorption coefficient to the solar spectrum than thiophene-based conjugated polymers.^[24] Therefore superior properties like high mobility and strong absorbance in a broad region could be expected for BDSe based copolymers, which possess big potential to develop ideal active material for PSCs. Recently, the research of a selenophene-based conjugated polymer in organic field-effect transistor device was reported by Kang *et al.*^[19,25,26] A high mobility of $\sim 0.1 \text{ cm}^2 \cdot \text{V}^{-1} \cdot \text{s}^{-1}$ improved to $4.97 \text{ cm}^2 \cdot \text{V}^{-1} \cdot \text{s}^{-1}$ was demonstrated for this selenophene-based conjugated polymer.^[19,27] At the same time, Yu *et al.* reported the synthesis of a series of copolymers containing selenopheno[3,4-b]selenophene and benzodiselenophene, which delivered power con-

* E-mail: whqbme@gmail.com, wlma@suda.edu.cn; Tel.: 0086-0512-65880945; Fax: 0086-0512-65882846

Received April 2, 2015; accepted May 8, 2015; published online June 10, 2015.

Supporting information for this article is available on the WWW under <http://dx.doi.org/10.1002/cjoc.201500270> or from the author.

version efficiency of 6.87% for polymer solar cell when blended with PC₇₁BM.^[28] And very recently, Ashraf *et al.* reported selenophene-based polymers, for which good field effect mobility of 1.6 cm²•V⁻¹•s⁻¹ and power conversion efficiency (PCE) of 7.6% for bulk-heterojunction solar cell was demonstrated,^[29] suggesting promising potential for BDSe based polymers in PSC applications.

As acceptor units, diketopyrrolopyrrole (DPP) and isoindigo (ID) have often been adopted in the design of D-A type polymers^[30-35] because of their excellent properties. Both DPP and ID possess the ability to achieve suitable lowest unoccupied molecular orbital (LUMO) for polymers to match well with the fullerene acceptors. Their strong electron withdrawing ability and their intrinsic energy band structure properties benefit the exciton dissociation.^[36-39] On the other hand, both units tend to provide broad absorption extending to the near-infrared region.^[35,40-42] Besides the influence on polymer's LUMO, DPP and ID can also help to lower the polymer's highest occupied molecular orbital (HOMO) level, hence increase the open circuit voltage (V_{OC}).^[43-45]

Herein in this work, we report new D-A type polymers, PBDS_e-DPP and PBDS_e-ID. Different from the polymers reported by Yu *et al.*, we have utilized a simple and easy-to-synthesize side-chain free unit BDSe as donor, and different unit DPP or ID as the acceptor. The thermal, photophysical, electrochemical and photovoltaic properties of the two polymers were investigated in detail. Both polymers show a broad absorption in the region of 350–750 nm, relatively low optical band gap, and suitable HOMO energy levels. And decent device performance can be achieved for both polymers as well, based on simple optimizations with additive.

Experimental

Materials and characterization

Tetrahydrofuran and toluene were dried over sodium/benzophenone ketyl and distilled before use. *N,N*-Dimethylformamide was distilled over CaH₂. Chloroform, methanol, and dichloromethane were used as received. All other chemicals were purchased from Sigma-Aldrich and used as received without further purification.

¹H NMR was performed on a Varian NMR system 300 MHz spectrometer with tetramethylsilane (TMS; δ 0) as the internal standard. Mass spectra were obtained by using a ThermoFisher Scientific GC/MS Trace-ISQ mass spectrometer. Gel permeation chromatography (GPC) analysis was carried out on a Waters 717–2410 instrument with polystyrenes as the standard and trichlorobenzene as eluant (flow rate 1.0 mL/min). The thermo gravimetric analysis (TGA) was conducted with a Perkin Elmer TGA4000 under nitrogen atmosphere at a heating rate of 10 °C/min. Ultraviolet-visible absorption spectra were recorded on a Perkin Elmer model

Lambda 750. The electrochemical cyclic voltammetry was carried out on a Zahner IM6 electrochemical workstation. Tapping-mode AFM images were obtained by a Veeco Multimode V instrument. Grazing incidence X-ray diffraction (GIXD) experiments were conducted at Shanghai Synchrotron Radiation Facility (SSRF) on diffraction beam line (BL14B1).

Synthesis of monomers and polymers

The synthesis of monomer 1,4-dibromo-2,5-di(octyn-1-yl)benzene (**2**) and benzo[1,2-b:4,5-b']bis(selenophene) (**3**): The compounds **2** and **3** were synthesized according to previous reference,^[41] experimental details can be found in the supporting information.

2,6-Bis(trimethylstannyl)benzo[1,2-b:4,5-b']bis(selenophene) (**4**): A solution of benzo[1,2-b:4,5-b']diselenophene (446 mg, 1.57 mmol) in anhydrous tetrahydrofuran (50 mL) was cooled to 0 °C, and left for 0.5 h. Then *n*-BuLi (2.4 mol/L, 1.3 mL) was added in dropwise in 10 min. The solution was stirred for 1 h at room temperature. The solution of trimethyltin chloride (3.45 mmol) in tetrahydrofuran (5 mL) was added to the mixture and then cooled to 0 °C and stirred for 2 h. Then the mixture was warmed up to room temperature in 2 h. Water (150 mL) was added to the mixture, which was then extracted with diethyl ether (30 mL × 3). The organic layer was dried with anhydrous Na₂SO₄. The solvent was removed by rotary evaporation and residue was purified by re-crystallization in ethanol to produce a white solid (700 mg, 73%). EI-MS *m/z*: 613.9 (M^+); ¹H NMR δ : 8.73 (s, 2H), 8.06 (s, 2H), 0.79 (s, 18H).

Synthesis of PBDS_e-DPP

In a 50 mL reaction tube, monomer **4** (220 mg, 0.22 mmol), monomer **5** (132 mg, 0.22 mmol), tri(*o*-tolyl)phosphine (20 mg, 0.08 mmol) and Pd₂(dba)₃ (10 mg, 0.001 mmol) were added under a nitrogen atmosphere. Then anhydrous toluene (6 mL) was injected into the reaction tube through a syringe. After being stirred for 12 h at 110 °C, the reaction mixture was cooled down to room temperature and then precipitated in methanol (130 mL). The precipitate was filtered and repeatedly washed with methanol (200 mL, 24 h), hexane (200 mL, 24 h) and chloroform (200 mL, 10 h) in a Soxhlet apparatus. The chloroform fraction was concentrated and precipitated in methanol. The precipitate was filtered and dried in a vacuum for 24 h at 90 °C. PBDS_e-DPP was obtained as dark green solid (130 mg, 52.7%). GPC: M_n = 8.0 kg/mol; poly dispersity index (PDI) = 1.79. ¹H NMR (300 MHz, CDCl₃) δ : 7.98–6.98 (br, 10H, ArH), 4.24 (br, 4H), 2.60–2.37 (br, 2H), 1.80–1.27 (br, 64H), 1.27–0.81 (br, 12H).

Synthesis of PBDS_e-ID

PBDS_e-ID was prepared from monomer **4** (220 mg, 0.22 mmol) and monomer **6** (138 mg, 0.22 mmol) by using the same method which was used for PBDS_e-DPP. A green solid was obtained with a yield of 50.0% (125

mg). GPC: $M_n=9.8$ kg/mol; PDI=2.40. $^1\text{H NMR}$ (300 MHz, CDCl_3) δ : 9.15–9.30 (br, 2H), 7.85–7.90 (br, 2H), 6.90–7.25 (br, 6H), 3.0–2.50 (br, 6H), 1.95–1.50 (br, 64H), 1.50–0.81 (br, 12H).

Fabrication and characterization

Polymer solar cells were fabricated with a general structure of ITO/PEDOT:PSS (40 nm)/polymer:PCBM/LiF (0.6 nm)/Al (100 nm). Patterned ITO glass substrates were cleaned by ultrasonic treatment with detergent, acetone, deionized water and isopropyl alcohol, respectively, and further treated with UV-ozone for 10 min to remove organic residue. A thin film of PEDOT:PSS (40 nm) was spin-coated on ITO substrates and annealed at 150 °C for 10 min. Blends of PBDSe-DPP (or PBDSe-ID) and PC_{61}BM of different ratios were dissolved in chloroform containing 10% (*V/V*) dichlorobenzene (DCB) (the optimal parameters, 5 mg polymer, 20 mg PC_{61}BM , and 1 mL solvent), filtered through a 0.45 mm poly(tetrafluoroethylene) filter, spin-coated at different speeds for 40 s. 0.6 nm LiF (0.2 Å/s) and 100 nm Al (2 Å/s) layers were then thermally evaporated on the active layer at a pressure of 1.0×10^{-6} mbar through a shadow mask (active area 7.25 mm^2). The current density-voltage characteristics of the photovoltaic cells were measured using a Keithley 2400 (*I-V*) digital source meter under a simulated AM 1.5G solar irradiation at $100 \text{ mW} \cdot \text{cm}^{-2}$ (Newport, Class AAA solar simulator, 94023A-U). The light intensity was calibrated by a certified Oriel Reference Cell (91150V).

Hole-only devices were fabricated to measure the hole-mobility of polymers by the space charge limited current (SCLC) method, with structure ITO/PEDOT/polymer:PCBM/ MoO_3 /Al. The hole-mobility is deter-

mined by fitting the dark current to the model of a single carrier SCLC, which is described by the following equation.^[33]

$$J = \frac{9}{8} \varepsilon_0 \varepsilon_r \mu_h \frac{V^2}{d^3}$$

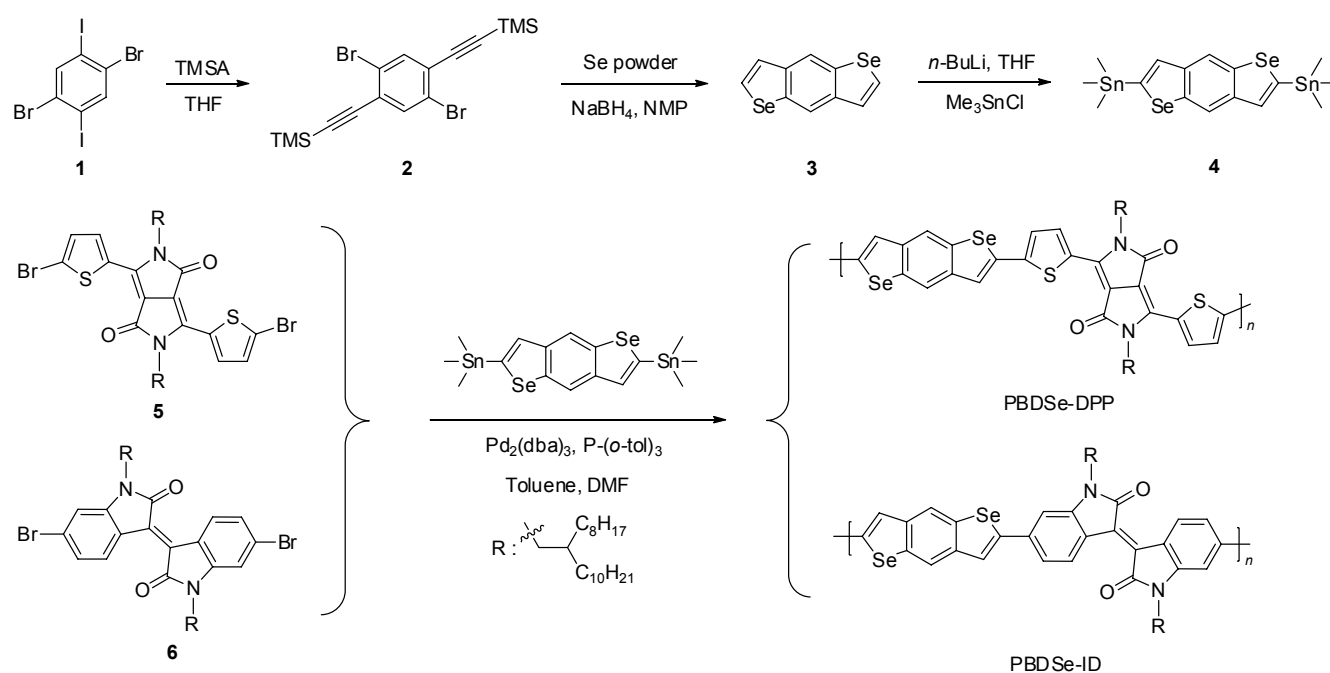
where J is the current, μ_h is the zero-field mobility, ε_0 is the permittivity of free space, ε_r is the relative permittivity of the material, d is the thickness of the active layer, and V is the effective voltage. The effective voltage can be obtained by subtracting the built-in voltage (V_{bi}) and the voltage drop (V_s) from the substrate's series resistance from the applied voltage (V_{appl}), $V = V_{\text{appl}} - V_{\text{bi}} - V_s$.

Results and Discussion

Synthesis and thermal properties

The synthetic routes for the monomers and polymers are illustrated in Scheme 1. Compounds **2** and **3** were prepared according to literature.^[46] Compound **2** was accomplished by substituting the iodine atom with TMS in compound **1**. Compound **3**, benzo[1,2-*b*:4,5-*b'*]bis(selenophene), was synthesized based on the ring closing reaction of compound **2**. Monomer **4** was obtained based on the reaction using compound **3**, chlorotrimethylstannane and *n*-BuLi in dried THF. Compounds **5** and **6** were synthesized according to literature.^[40,41] Since no side-chain engineering was carried out for the donor unit, which simplifies the synthesis procedure for the polymers PBDSe-DPP and PBDSe-ID. To ensure sufficient solubility for both polymers, long side-chain 2-octyldodecyl (**R**) was adopted in both DPP and ID acceptor units.

Scheme 1 The synthetic routes of different monomers and copolymers



The molecular weight and poly dispersity index (PDI) of the resultant polymers PBDSe-DDP and PBDSe-ID, synthesized by Stille poly condensations, are listed in Table 1. Both polymers show relatively good solubility since they can be dissolved in common solvents like tetrahydrofuran, chloroform and chlorobenzene, at room temperature. At the same time, the molecular weight is very low which may affect the cell performance as higher molecular weight polymer usually has a better device performance.

Table 1 Molecular weights and thermal properties of the polymers

Polymer	M_p^a /($\text{kg}\cdot\text{mol}^{-1}$)	M_w^a /($\text{kg}\cdot\text{mol}^{-1}$)	PDI ^a	T_d^b /°C
PBDSe-DPP	8.6	14.3	1.79	389
PBDSe-ID	10.3	23.5	2.40	398

^a Determined by GPC using polystyrene standards and THF as eluent. ^b 5% weight loss temperatures measured by TGA under nitrogen.

The thermal stability of the two polymers was examined by TGA and their results are listed in Table 1. As shown in Figure 1, both polymers show good thermal stability with onset decomposition temperature (T_d) corresponding to 5% weight loss at 389 °C and 398 °C respectively, which is adequate for normal applications in PSCs.

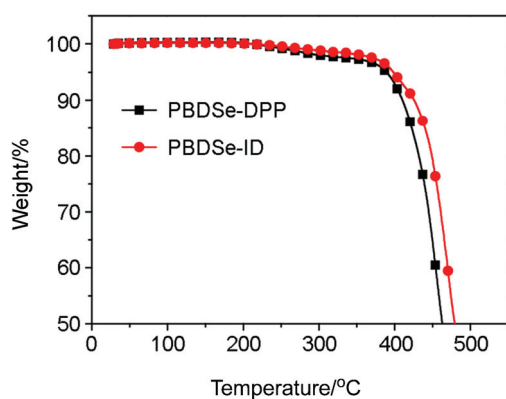


Figure 1 TGA curves of copolymers at scan rate of 10 °C/min under N_2 atmosphere.

Photophysical and electrochemical properties

The photophysical properties of the polymers were investigated by UV-Vis spectroscopy as shown in Figure 2, and the key parameters are summarized in Table 2. Both polymers absorb solar photons in a broad range extending to the near infrared region. Especially the PBDSe-DPP extends its absorption to the near infrared range approaching 800 nm. Both polymers show two distinct absorption bands in solution and film states. The first absorption band is located in the violet region with the absorption peak ($\lambda_{s,\text{max}}$) at 409 nm and 374 nm for PBDSe-DPP and PBDSe-ID respectively, which can be identified with a delocalized excitonic π - π^* transition.

The second absorption band with $\lambda_{s,\text{max}}$ at 695 and 674 nm respectively, can be attributed to a localized transition between donor-acceptor charge transfer states.^[47] Compared to the solution sample, both polymer films showed narrowed absorption at the second absorption band. This phenomenon could be the result of the enhanced inter-chain interaction in the solid films, which is most likely related to the increased π - π stacking of the backbones in the film.^[48,49]

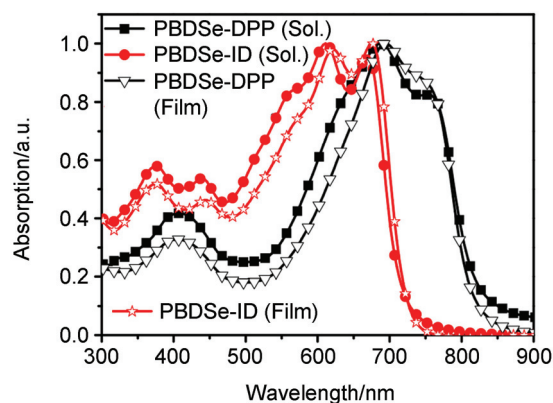


Figure 2 Absorption spectra of polymers in chloroform solution and thin films.

The cyclic voltammetry measurement was used to study the electrochemical behavior of the polymers. The corresponding cyclic voltammetry curves and data of PBDSe-DPP and PBDSe-ID films are shown in Figure S1 (see the Supporting Information) and summarized in Table 2. The onset potential of oxidation (E_{ox}) is observed to be 1.02 and 1.20 eV for PBDSe-DPP and PBDSe-ID, respectively. The HOMO energy levels of PBDSe-DPP and PBDSe-ID were calculated to be -5.15 eV and -5.31 eV, respectively ($E_{\text{HOMO}} = -(E_{\text{onset}}^{\text{ox}} - 0.69) - 4.8$ eV), which suggests a relatively ideal V_{OC} . These deep HOMO energy levels are due to the introduction of the acceptor unit in the backbone. PBDSe-ID shows a deeper HOMO level than PBDSe-DPP, predicting a higher V_{OC} of PSCs. The LUMO energy levels of PBDSe-DPP and PBDSe-ID were measured to be -3.59 eV and -3.61 eV ($E_{\text{LUMO}} = -(E_{\text{onset}}^{\text{red}} - 0.69) - 4.8$ eV) determined by the redox onset (-0.48 and -0.5 eV). Both can provide sufficient driving force (>0.3 eV) for the exciton dissociation compared to the LUMO energy level (-4.0 eV) of PC_{61}BM . These results indicate that the HOMO and LUMO energy levels of our new polymers match well with fullerene derivatives for photovoltaic application.

The energy level alignment diagram of the two polymers along with the PC_{61}BM , PEDOT:PSS and electrodes is shown in Figure 3.

Theoretical calculations

In general, polymer coplanarity is considered important to influence the intermolecular packing, the device fill factor (FF) and the photovoltaic performance. A

Table 2 Optical and electrochemical properties of polymers

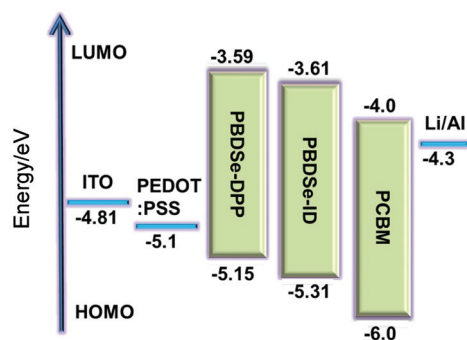
Polymer	λ_{\max}/nm		$\lambda_{\text{onset}}/\text{nm}$		$E_{\text{g}}^{\text{opt } a}/\text{eV}$	HOMO ^b /eV	LUMO ^b /eV	$E_{\text{g}}^{\text{EC}}/\text{eV}$
	Solution	Film	Solution	Film				
PBDSe-DPP	683	695	622	634	1.46	-5.15	-3.59	1.56
PBDSe-ID	668	674	731	776	1.68	-5.31	-3.61	1.70

^a $E_{\text{g}}^{\text{opt}}$ s were estimated from the onset of UV-vis spectra of films. ^b The HOMO/LUMO^(elec) energy level is calculated by equation HOMO/LUMO = $-(E_{\text{ox}}/E_{\text{red}} - 0.70) - 4.80$ eV.

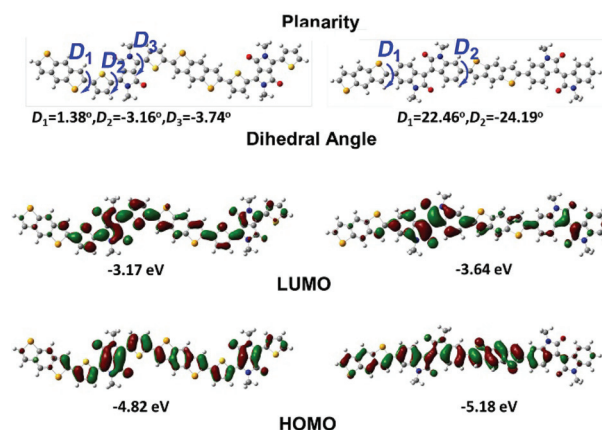
Table 3 Photovoltaic properties of different polymers blended with PC₆₁BM ($w/w=1:4$), when additive DIO or DCB is used or not

Polymer	V_{oc}/V	$J_{\text{sc}}/(\text{mA}\cdot\text{cm}^{-2})$	FF/%	PCE/%	$R_{\text{s}}/(\Omega\cdot\text{cm}^2)$	$R_{\text{sh}}/(\text{k}\Omega\cdot\text{cm}^2)$
PBDSe-DPP	0.70	5.65	66.8	2.64	98.7	22.4
PBDSe-DPP ^a	0.70	7.11	65.7	3.27	89.8	16.3
PBDSe-DPP ^b	0.69	9.25	58.3	3.72	51.4	11.2
PBDSe-ID	0.75	2.84	67.8	1.44	364	30.4
PBDSe-ID ^a	0.74	5.27	41.6	1.62	86.2	6.71
PBDSe-ID ^b	0.73	6.23	55.6	2.53	217	13.0

^a with additive 2% DIO. ^b with additive 10% DCB.

**Figure 3** Energy diagram for HOMO-LUMO energy levels of the two polymers.

suitable band gap and finely tuned energy levels are beneficial for the device short circuit current (J_{SC}) and V_{OC} .^[47,50] To get insight into the planarity of the molecular architecture and the energy levels, we performed the density functional theory (DFT) calculations at the B3LYP/6-31GD level on model compounds using the Gaussian 09 program suite. Solvent effect was taken into account by using a proper dielectric constant of 2.4. To simplify the calculation, two repeating unit of each polymer was subject to calculation, with alkyl chains replaced by CH_3 groups. The key dihedral angles between the donor and acceptor unit of the backbone were measured to compare the distortions. The two polymers show good backbone planarity as demonstrated by DFT calculations. As shown in Figure 4, the key dihedral angles of D_1 , *i.e.* 1.38° for selenophene-thiophene in PBDSe-DPP and 22.46° for selenophene-benzene in PBDSe-ID are determined respectively. The smaller dihedral angles of PBDSe-DPP imply that the planarity is better performed. The theoretically calculated HOMO level and band gap are -4.82 eV and 1.65 eV for PBDSe-DPP and -5.18 eV and 1.54 eV for PBDSe-ID. These calculations are consistent with the results obtained from CV and optical measurements.

**Figure 4** Characterizations of planarity, key dihedral angles and the HOMO/LUMO levels of the polymers by DFT calculations.

Photovoltaic property and film morphology

The solar cells employing PBDSe-DPP or PBDSe-ID as the electron donor and PC₆₁BM as the electron acceptor were fabricated, with device configuration of ITO/PEDOT:PSS/Polymer:PC₆₁BM/LiF/Al. The current density-voltage ($J-V$) curves of the solar cells are presented in Figure 5. The specific parameters of the photovoltaic performances are summarized in Table 3. The best power conversion efficiencies (PCEs) were obtained for both polymer-based devices when the ratio 1:4 (w/w) of polymer:PC₆₁BM was adopted. Although the original solar cells present moderate PCEs, relatively high V_{OC} s (0.7 and 0.75 V) and FF (0.67 and 0.68) have been accomplished for the two polymers, which is consistent with the results and analysis of the cyclic voltammetry measurement. PBDSe-DPP delivers higher J_{SC} than PBDSe-ID due to its broader absorption extending into the infrared regime. To improve the device performance, additives were applied in the solvent systems. Significant improvement of the device performance is observed when additive dichlorobenzene (DCB)

or 1,8-diiodooctane (DIO) is applied. Notably, the J_{SC} shows an enhancement of 64% (from 5.65 to 9.25 mA/cm²) when DCB is used in the PBDS_e-DPP:PC₆₁BM system, with steady V_{OC} and only slightly decreased FF, offering the highest PCE of 3.72% (Figure 5). Huge improvement is also observed when DIO is used as the additive, which delivers an improved PCE of 3.27%. The more balanced parameter values of the device with additive DCB provide the best performance (Table 3). For the PBDS_e-ID:PC₆₁BM system, even larger improvement (~120%) of J_{SC} is observed with additive DCB, while keeping V_{OC} steady. However, greatly decreased FFs are observed for devices treated with additive DCB or DIO, offering moderate PCEs of 2.53% and 1.62%, respectively (Table 3). Relatively high V_{OC} s were obtained for both PBDS_e-DPP and PBDS_e-ID based devices (Table 3), due to their deep HOMO levels. Specifically, the PBDS_e-ID provided a slightly higher V_{OC} than PBDS_e-DPP, which could be attributed to the deeper HOMO of PBDS_e-ID. However, moderate overall J_{SC} s were obtained for both polymer based devices, and consequently a moderate overall device performance compared with other ideal polymer based devices. This could result from the fact that the intermolecular arrangements and resulting energy landscapes at the donor-acceptor interface are unfavourable for charge separation.^[51] The external quantum efficiency (EQE) spectra of the solar cells based on both polymers are depicted in Figure 6. Both polymer-based devices showed broad photon response extending into the near infrared region, which is consistent with the absorption spectra. And from the EQE spectra, relatively low (~15% lower) integrating J_{SC} s are obtained for both polymer-based devices, compared to their measured J_{SC} values, which could result from the degradation of the polymer/device in atmosphere in the measurement.

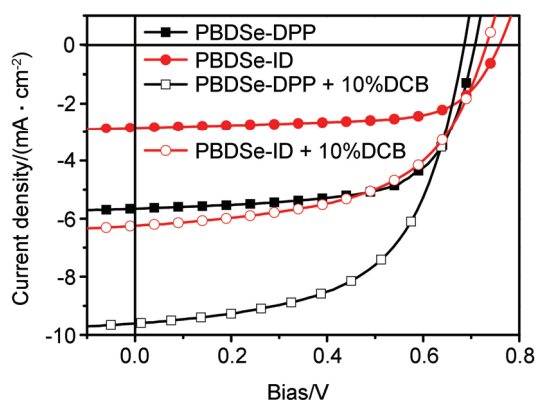


Figure 5 J - V curves of polymer:PC₆₁BM-based devices, with and without 10% DCB additive, processed with chloroform.

To further understand the varying performance of the devices, the surface morphology of the PBDS_e-DPP:PC₆₁BM and PBDS_e-ID:PC₆₁BM blend films (with and without additive DCB/DIO) were investigated by

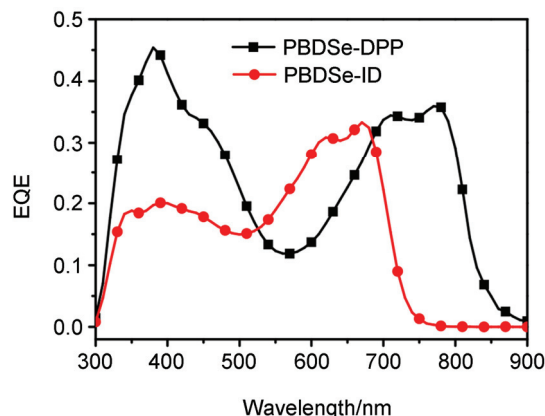


Figure 6 EQE curves of the photovoltaic devices based on PBDS_e-DPP and PBDS_e-ID with 10% DCB additive.

atomic force microscopy (AFM), as shown in Figure 7 and Figure S2. The root mean square (RMS) roughness of 1.52 nm was determined for the PBDS_e-DPP:PC₆₁BM film. Smoother surface morphologies with RMS 1.26 and 1.0 nm were observed when additives DIO and DCB were used, respectively, which is consistent with the corresponding results of the device performance. Again obvious improvement of the film morphology was observed when additives were used in the PBDS_e-ID:PC₆₁BM blend films (Figure 7d, 7e and 7f). Much smaller domain size and lower RMS were achieved when additives were applied. To sum up, overall better surface morphology and smaller domain size are obtained for the PBDS_e-DPP:PC₆₁BM blend compared to the PBDS_e-ID:PC₆₁BM blend, and both blend systems can be effectively improved with additive DIO/DCB, which could have contributed to the device performances. The overall better film morphology of the PBDS_e-DPP:PC₆₁BM blend could partially account for its better device performance, compared to the PBDS_e-ID:PC₆₁BM device. As more direct information to evaluate the blend quality, the series resistance (R_s) and shunt resistance (R_{sh}) of the devices are summarized in Table 3. For the PBDS_e-DPP system, both R_s and R_{sh} decrease when additive DIO or DCB is used, which could mainly account for the increased J_{SC} and decreased FF respectively, and are consistent with the device performances. For the PBDS_e-ID system, decreased R_s and R_{sh} are observed as well for both additive systems. However less enhancement of PCE is obtained compared to the PBDS_e-DPP system, due to the lower J_{SC} and drastically decreased FF which could mainly be caused by the much faster dropped R_{sh} .

In addition, GIXD was used to study the molecular arrangement in blend film of the two polymers. However, disordered packing and random orientation nature in blend film can be concluded from the observed weak diffractions for both polymers (Figure S3), which is consistent with the observed relatively low J_{SC} s. And it could result in the relatively moderate charge carrier mobility of 1.5×10^{-4} cm²·V⁻¹·s⁻¹ and 1.3×10^{-4} cm²·V⁻¹·s⁻¹ for PBDS_e-DPP and PBDS_e-ID respec-

tively, determined by fitting the slope of the $J^{1/2}$ - V curves (Figure S4) according to SCLC measurement.

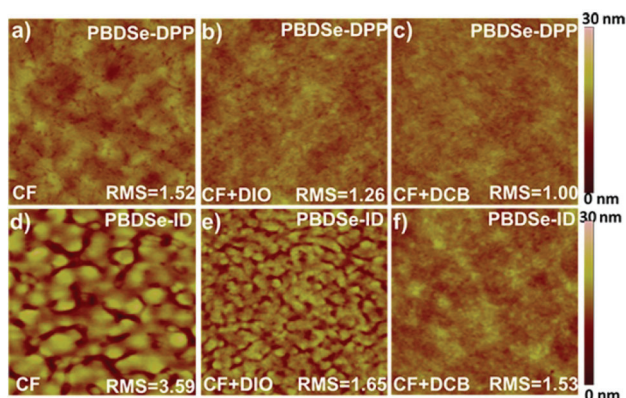


Figure 7 AFM height images ($2.0\ \mu\text{m} \times 2.0\ \mu\text{m}$) of different active layers. (a–c) PBDS-e-DPP/PC₆₁BM with none, 2% DIO and 10% DCB additive, (d–f) PBDS-e-ID/PC₆₁BM with none, 2% DIO and 10% DCB additive.

Conclusions

To summarize, based on the side-chain free donor unit BDSe and acceptor unit DPP/ID, two new D-A type semiconducting polymers PBDS-e-DPP and PBDS-e-ID were design and synthesized for photovoltaic application. Both polymers exhibited good thermal stability, desired band-gaps and suitable HOMO/LUMO levels. Relatively high V_{OC} (0.7 and 0.75 V) and FF (>65%) were demonstrated for both polymer based solar cells, and decent PCEs of 3.72% and 2.53% were achieved by utilizing additive with only simple optimizing consideration. We believe that better device performance can be accomplished with the new polymers when suitable solvent/additive system is adopted. And this class of BDSe-based polymers possess the potential to be good alternatives for active material in photovoltaic application.

Acknowledgement

This work was supported by the National High Technology Research and Development Program of China (863 Program) (Grant No. 2011AA050520), the National Natural Science Foundation of China (Grant no. 61176054), the China Postdoctoral Science Foundation (Grant No. 2014M550302 and 1302015A), the Project Sponsored by the Scientific Research Foundation for the Returned Overseas Chinese Scholars (State Education Ministry), and the Priority Academic Program Development of Jiangsu Higher Education Institutions.

References

[1] Yu, G.; Gao, J.; Hummelen, J.; Wudl, F.; Heeger, A. *Science* **1995**, *270*, 1789.

- [2] Thompson, B. C.; Fréchet, J. M. J. *Angew. Chem., Int. Ed.* **2008**, *47*, 58.
- [3] Chen, J.; Cao, Y. *Acc. Chem. Res.* **2009**, *42*, 1709.
- [4] Cheng, Y.-J.; Yang, S.-H.; Hsu, C.-S. *Chem. Rev.* **2009**, *109*, 5868.
- [5] Li, Y. *Acc. Chem. Res.* **2012**, *45*, 723.
- [6] Dennler, G.; Scharber, M. C.; Brabec, C. J. *Adv. Mater.* **2009**, *21*, 1323.
- [7] Kim, J. Y.; Lee, K.; Coates, N. E.; Moses, D.; Nguyen, T.-Q.; Dante, M.; Heeger, A. J. *Science* **2007**, *317*, 222.
- [8] Zhou, H.; Yang, L.; You, W. *Macromolecules* **2012**, *45*, 607.
- [9] Liu, L.; Bavel, S. V.; Wen, S.; Yang, X.; Loos, J. *Chin. J. Chem.* **2013**, *31*, 731.
- [10] Bian, L.; Zhu, E.; Tang, J.; Tang, W.; Zhang, F. *Prog. Polym. Sci.* **2012**, *37*, 1292.
- [11] Wang, Y.; Wei, W.; Liu, X.; Gu, Y. *Sol. Energ. Mat. Sol. C.* **2012**, *98*, 129.
- [12] Zhang, Z. G.; Wang, J. *J. Mater. Chem.* **2012**, *22*, 4178.
- [13] Son, H. J.; He, F.; Carsten, B.; Yu, L. *J. Mater. Chem.* **2011**, *21*, 18934.
- [14] Hou, J.; Park, M.-H.; Zhang, S.; Yao, Y.; Chen, L.-M.; Li, J.-H.; Yang, Y. *Macromolecules* **2008**, *41*, 6012.
- [15] Liang, Y.; Xu, Z.; Xia, J.; Tsai, S.-T.; Wu, Y.; Li, G.; Ray, C.; Yu, L. *Adv. Mater.* **2010**, *22*, E135.
- [16] Park, S. H.; Roy, A.; Beaupre, S.; Cho, S.; Coates, N.; Moon, J. S.; Moses, D.; Leclerc, M.; Lee, K.; Heeger, A. J. *Nat. Photonics* **2009**, *3*, 297.
- [17] Huang, Y.; Guo, X.; Liu, F.; Huo, L.; Chen, Y.; Russell, T. P. C.; Han, C.; Li, Y.; Hou, J. *Adv. Mater.* **2012**, *24*, 3383.
- [18] Li, Z.; Zhang, Y.; Tsang, S.-W.; Du, X.; Zhou, J.; Tao, Y.; Ding, J. *J. Phys. Chem. C* **2011**, *115*, 18002.
- [19] Khim, D.; Lee, W.-H.; Baeg, K.-J.; Kim, D.-Y.; Kang, I.-N.; Noh, Y.-Y. *J. Mater. Chem.* **2012**, *22*, 12774.
- [20] Lee, W. H.; Lee, S. K.; Son, S. K.; Choi, J. E.; Shin, W. S.; Kim, K.; Lee, S. H.; Moon, S. J.; Kang, I. N. *J. Polym. Sci. Part A: Polym. Chem.-UK* **2012**, *50*, 551.
- [21] Takimiya, K.; Kunugi, Y.; Konda, Y.; Niihara, N.; Otsubo, T. *J. Am. Chem. Soc.* **2004**, *126*, 5084.
- [22] Chen, Z.; Lemke, H.; Albert-Seifried, S.; Caironi, M.; Nielsen, M. M.; Heeney, M.; Zhang, W.; McCulloch, I.; Siringhaus, H. *Adv. Mater.* **2010**, *22*, 2371.
- [23] Wang, J.; Ye, H.; Li, H.; Mei, C.; Ling, J.; Li, W.; Shen, Z. *Chin. J. Chem.* **2013**, *31*, 1367.
- [24] Ballantyne, A. M.; Chen, L.; Nelson, J.; Bradley, D. D. C.; Astuti, Y.; Maurano, A.; Shuttle, C. G.; Durrant, J. R.; Heeney, M.; Duffy, W.; McCulloch, I. *Adv. Mater.* **2007**, *19*, 4544.
- [25] Lee, W.-H.; Son, S. K.; Kim, K.; Lee, S. K.; Shin, W. S.; Moon, S.-J.; Kang, I.-N. *Macromolecules* **2012**, *45*, 1303.
- [26] Lee, W.-H.; Lee, S.-K.; Shin, W.-S.; Moon, S.-J.; Lee, S.-H.; Kang, I.-N. *Sol. Energ. Mat. Sol. C.* **2013**, *110*, 140.
- [27] Kang, I.; An, T. K.; Hong, J.-A.; Yun, H.-J.; Kim, R.; Chung, D. S.; Park, C. E.; Kim, Y.-H.; Kwon, S.-K. *Adv. Mater.* **2013**, *25*, 524.
- [28] Saadeh, H. A.; Lu, L.; He, F.; Bullock, J. E.; Wang, W.; Carsten, B.; Yu, L. *ACS Macro Lett.* **2012**, *1*, 361.
- [29] Ashraf, R. S.; Meager, I.; Nikolka, M.; Kirkus, M.; Planells, M.; Schroeder, B. C.; Holliday, S.; Hurhangee, M.; Nielsen, C. B.; Siringhaus, H.; McCulloch, I. *J. Am. Chem. Soc.* **2015**, *137*, 1314.
- [30] Zhou, E.; Yamakawa, S.; Tajima, K.; Yang, C.; Hashimoto, K. *Chem. Mater.* **2009**, *21*, 4055.
- [31] Bijleveld, J. C.; Gevaerts, V. S.; Di Nuzzo, D.; Turbiez, M.; Mathijssen, S. G.; De Leeuw, D. M. M.; Wienk, M.; Janssen, R. A. *Adv. Mater.* **2010**, *22*, E242.
- [32] Bijleveld, J. C.; Verstrijden, R. M.; Wienk, M. M.; Janssen, R. A. *J. Mater. Chem.* **2011**, *21*, 9224.
- [33] Kim, G.; Kang, S. J.; Dutta, G. K.; Han, Y. K.; Shin, T. J.; Noh, Y. Y.; Yang, C. *J. Am. Chem. Soc.* **2014**, *136*, 9477.

- [34] Deng, P.; Zhang, Q. *Polym. Chem.-UK* **2014**, *5*, 3298.
- [35] Deng, P.; Xiong, J.; Li, S.; Wu, Y.; Yang, J.; Zhang, Q. *Chin. J. Chem.* **2014**, *32*, 521.
- [36] Qu, S.; Tian, H. *Chem. Commun.* **2012**, *48*, 3039.
- [37] Lei, T.; Cao, Y.; Fan, Y.; Liu, C.-J.; Yuan, S.-C.; Pei, J. *J. Am. Chem. Soc.* **2011**, *133*, 6099.
- [38] Walker, B.; Tamayo, A. B.; Dang, X. D.; Zalar, P.; Seo, J. H.; Garcia, A.; Tantiwiwat, M.; Nguyen, T. Q. *Adv. Funct. Mater.* **2009**, *19*, 3063.
- [39] Wang, E.; Ma, Z.; Zhang, Z.; Vandewal, K.; Henriksson, P.; Inganäs, O.; Zhang, F.; Andersson, M. R. *J. Am. Chem. Soc.* **2011**, *133*, 14244.
- [40] Nielsen, C. B.; Turbiez, M.; McCulloch, I. *Adv. Mater.* **2013**, *25*, 1859.
- [41] Kronemeijer, A. J.; Gili, E.; Shahid, M.; Rivnay, J.; Salleo, A.; Heeney, M.; Sirringhaus, H. *Adv. Mater.* **2012**, *24*, 1558.
- [42] Irimia-Vladu, M.; Glowacki, E. D.; Troshin, P. A.; Schwabegger, G.; Leonat, L.; Susarova, D. K.; Krystal, O.; Ullah, M.; Kanbur, Y.; Bodea, M. A.; Razumov, V. F.; Sitter, H.; Bauer, S.; Sariciftci, N. S. *Adv. Mater.* **2012**, *24*, 375.
- [43] Stalder, R.; Mei, J.; Reynolds, J. R. *Macromolecules* **2010**, *43*, 8348.
- [44] Mei, J.; Graham, K. R.; Stalder, R.; Reynolds, J. R. *Org. Lett.* **2010**, *12*, 660.
- [45] Li, W.; Lee, T.; Oh, S. J.; Kagan, C. R. *ACS Appl. Mater. Inter.* **2011**, *3*, 3874.
- [46] Kashiki, T.; Shinamura, S.; Kohara, M.; Miyazaki, E.; Takimiya, K.; Ikeda, M.; Kuwabara, H. *Org. Lett.* **2009**, *11*, 2473.
- [47] Yuan, J.; Huang, X.; Dong, H.; Lu, J.; Yang, T.; Li, Y.; Gallagher, A.; Ma, W. *Org. Electron.* **2013**, *14*, 635.
- [48] Zou, Y.; Gendron, D.; Neagu-Plesu, R.; Leclerc, M. *Macromolecules* **2009**, *42*, 6361.
- [49] Liu, B.; Zou, Y.; Peng, B.; Zhao, B.; Huang, K.; He, Y.; Pan, C. *Polym. Chem.-UK* **2011**, *2*, 1156.
- [50] Huo, L.; Zhang, S.; Guo, X.; Xu, F.; Li, Y.; Hou, J. *Angew. Chem.* **2011**, *123*, 9871.
- [51] Graham, K. R.; Cabanetos, C.; Jahnke, J. P.; Idso, M. N.; El Labban, A.; Ngongang Ndjawa, G. O.; Heumueller, T.; Vandewal, K.; Salleo, A.; Chmelka, B. F.; Amassian, A.; Beaujuge, P. M.; McGehee, M. D. *J. Am. Chem. Soc.* **2014**, *136*, 9608.

(Pan, B.; Fan, Y.)